Computational Simulation of Electroosmotic Flow Using Immersed Boundary Method

C.A. Saleel[1], A. Shaija[2] and S. Jayaraj[3]
Mechanical Engineering Department, National Institute of Technology, Calicut, Kerala-673601, India

ABSTRACT

Several fluid movement techniques in microchannel have been discussed in the past, the most recent technique is by applying an electric field to a fluid enclosed in a microchannel (*viz* electroosmotic flow). An immersed boundary method (IBM) is a methodology to deal with a body in the computational domain having complex or simple boundary which does not necessarily have to conform a Cartesian grid. The present study is an IBM based numerical investigation of two-dimensional transient electroosmotic flows in a microchannel populated with rectangular blocks to constrict the flow which eventually aims a short mixing channel. Electroosmotic potential, leads to the formation of Electrical Double Layer (EDL), is governed by Poisson-Boltzmann equation and is solved by PSOR method. The hyperbolic non-linearity associated with this equation is suitably tackled by the Taylor series expansion (neglecting the higher order terms). The electroosmotic flow is governed by the continuity equation impregnated with a mass source term and the Navier-Stokes equation along with electroosmotic forcing component and momentum forcing function. Both momentum forcing and mass source term are made active in the vicinity of the immersed body to satisfy the no-slip boundary condition on the same and also to satisfy the continuity for the cell containing the immersed boundary. Numerical solution of the governing equations are made possible by employing an ADI approximate factorization technique clubbed with powerful and accurate Tri-Diagonal Matrix Algorithm (TDMA). The results are generated in terms of α, the ionic energy parameter and β, which relates ionic energy parameter, characteristic length (microchannel height in the present study) and Debye-Huckel parameter.

Keywords: Electroosmotic Flow, Electrical Double Layer, Immersed Boundary Method, Momentum Forcing Function, Mass source term

1. INTRODUCTION

The talent to handle complex geometries has been one of the foremost issues in computational fluid dynamics because most engineering problems have complex geometries. So far, two different approaches to simulate complex flow have been developed, namely, the unstructured grid method and IBM. The primary issues raised during the handling of complex geometries in conventional fluid dynamics simulations are

(i) Ability to handle complex geometries: even though the unstructured grid is inherently better suited for complex geometries, grid quality can deteriorate with increasing complexity in the geometry.

*Corresponding author. [1]ahamedsaleel@nitc.ac.in; [2]shaija@nitc.in; [3]sjayaraj@nitc.ac.in http://www.nitc.ac.in

(ii) Accuracy: of the numerical solution, i.e., its closeness to the exact solution, depends only on the grid generation process, and not on the solution methods employed to solve the discretized equations. The solution method determines whether we are successful in obtaining a solution, and how much time and effort it will cost us; but it does not determine the final answer.

(iii) Computational Efficiency: use of structured curvilinear body conformal grids will necessitate the presence of additional terms associated with grid transformations. Also the use of unstructured grids will make numerical methods not amenable to powerful line iterative techniques.

The afore mentioned issues are mainly raised from the process of grid generation. The IBM greatly simplifies the task of grid generation by eliminating all the difficulties associated with the same. In IBM, the presence of a complex boundary is replaced by a time-spatially varying distribution of a forcing function as mentioned above, which is an extra term appears in governing equations either before or after the discretization. The boundary conditions on the surface are not imposed directly, instead the above said forcing function mimics the effect of the body/ boundary on the flow. In this work, an attempt is made to simulate electroosmotic flow in a constricted microchannel using the immersed boundary method. Recent developments in micro-fabrication technologies enabled a variety of miniaturized fluidic systems consisting of micro-nozzles, valves, pumps, and various other injection systems, which can be utilized in medical, pharmaceutical and defense applications. These micro-fluidics systems/devices require some fluid-solid interacting components or immersed boundaries to ease sample collection, separation, mixing of reagents which is the part of biological and chemical detection units with fluid pumping, flow control elements, and also of the necessary electronics on a single microchip. Altogether, the flow in microfluidic systems may be analyzed more easily using IBM.

1.1. Immersed boundary method

Fluids flows over complex geometries are very common in engineering problems, and the major difficulty arise in how to represent the body, its moving walls and its interaction with the fluid. The most accustomed approach is using Neumann and Dirichlet boundary conditions to represent the body geometry. Therefore, if the geometry is complex, treatment will have a hard and probably a complicated work. This difficulty grows up if the body has a poignant or deformable geometry. In short, treating the coupling of the structure deformations and the fluid flow poses a number of challenging problems in numerical simulations. Both the unstructured grid method and IBM are equally popular for simulating the fluid flow involving complex geometries.

In addition to the above mentioned two methods, some authors have proposed different methods to treat this kind of problem. For example, Harlow and Welch [1] proposed the marker and cell (MAC) approach. In this method the fluid region on one side of the boundary is identified by markers, while on the other side of the boundary, which can be fluid or solid, is identified by another marker. It requires huge storage space and CPU time.

The phrase "immersed boundary method" was first appeared in literature in reference to a method developed by Peskin [2]. A force term added to the Navier-Stokes equation is in charge to promote the interaction between fluid-solid interactions. Variety of innovative ideas have been proposed later to calculate this force term and each initiative leads to a particular kind of immersed boundary technique. Originally this technique was used to simulate cardiac mechanics and associated blood flow. The legendary feature of this method was that, the entire simulation was carried out on a Cartesian grid, which did not conform to the geometry of the heart and a novel procedure was imitated for imposing the effect of the immersed boundary (IB) on the flow. The boundary conditions are imposed not in a straight forward manner in IBM. Since Peskin's introduction about this method, there arise numerous modifications and refinements to this technique. Now a number of variants of this approach exist. The major advantages of the Immersed Boundary Method include savings in computer memory and CPU time. Also easy grid generation is possible with IBM compared to the unstructured grid method. Even moving boundary problems can be handled using IBM without regenerating grids in time, unlike the structured grid method. It is to be noted that generation of body conformal grids (structured or unstructured) is habitually very cumbersome.

The key factor in developing an IB algorithm is the way of imposition of boundary conditions on the IB and the same distinguishes one IB method from another. In the former approach, which is termed as “continuous forcing approach”, the forcing function is incorporated into the conservation equations before discretization. In the latter approach (which can be termed the “discrete forcing approach”), the forcing function is introduced after the equations are discretized. An attractive feature of the continuous forcing approach is that it is formulated independent of the underlying spatial discretization. On the other hand, the discrete forcing approach very much depends on the discretization method. However, this allows direct control over the numerical accuracy, stability, and discrete conservation properties of the solver as cited by Mittal and Iaccarino [3].

The merits of continuous forcing approach are its attractiveness for problems with elastic boundaries, closeness to the physics of the problem; hence relatively easy to conjure up the realistic flow problems especially high feasibility for successful simulation of biological and multiphase flows. The demerits of the aforementioned method include development of “stiff” numerical systems due to the presence of rigid Immersed Boundary in flow problems. Here satisfactory results have only been attained for low Reynolds number flows with moderate unsteadiness. Smoothing of the forcing function prohibits the sharp representation of the IB, which is not acceptable at high Reynolds numbers. The method also necessitates the computation in substantial amount of grid points located inside the body which simply results in unnecessary extra computation time. The merits of discrete forcing approach include

(i) Suitability for flows around rigid bodies,
(ii) Handling of higher Reynolds number flows,
(iii) Absence of stiffness or user defined parameters that can impact the stability of the method,
(iv) The ability to represent sharp IB by imposing the boundary conditions directly on the numerical scheme and
(v) Computation of flow variables inside a rigid body becomes unnecessary.

Where as, its demerits are the need for a pressure boundary condition on the IB and moving boundaries are harder to deal with than in continuous forcing IBMs. A review about IBMs encompassing all variants is presented by Mittal and Iaccarino [3]. Feedback forcing method is also applied to represent a solid body (Goldstein *et al.* [4]), which induced spurious oscillations and restricted the computational time step associated with numerical stability.

Yusof [5] proposed a different approach to evaluate the momentum forcing function in a spectral method, and his method does not require a smaller computational time step, which is an important benefit of this method over preceding methods. The discrete IB finite volume method (Kim *et al.* [6]) is used to simulate the present problem and is based on a staggered mesh together with a fractional step method. The obstruction is treated as an IB. Both momentum forcing and mass source are applied on the body surface or inside the body to suit the no-slip boundary condition on the IB and also to satisfy the continuity for the cell containing the IB. In this IBM, the choice of an accurate interpolation scheme satisfying the no-slip condition on the IB is very important.

1.2. Electroosmotic flow

The flow and associated transport phenomena in micro-channels have received increasing attention. The importance of micro-fluidic applications has been ascertained in recent review articles. Among various mechanisms to manipulate flow in micro-fluidic devices, electro-osmosis has emerged as a promising means, particularly under the highly viscous situations in which the Reynolds number is less than the unity. The term “Electro-osmotic flow (EOF) or Electro-osmosis” was first referred by Reuss [7] in a paper entitled ‘*Sur un nouvel effet de lé électricité galvanique*’ that appeared in the *Proceedings of the Imperial Society of Naturalists, Moscow*. In that paper, he demonstrated that water could be made to percolate through porous clay diaphragms by the application of an electric field. The mechanism behind the phenomena is unrelated to biological osmosis, which is, the flow of water across a semi-permeable membrane driven by a solute concentration gradient. Instead, the mechanism behind this observed mobility of water is as follows. Particles of clay and other silicate materials such as glass or silicon, acquire a surface charge when in contact with an electrolyte such as water due to chemical dissociation of surface ionic groups. The amount of this surface charge is determined by various factors but a typical value for silica–water interfaces is in the range of –4 to –60 milli-Coulomb per square meter. These fixed charges on the substrate attract the free charges in solution of unlike sign and repel those of like sign (the free charges in solution are ionic dissociation products of the water molecule itself as well as salt ions that even relatively pure water contains in bountiful amounts). This consequence in the formation of a thin (1–10 nm) charged region in the solute next to the substrate boundary known as the Debye layer. In the presence of an external electric field, the fluid in this Debye layer experiences a body force thereby acquiring momentum which is then transmitted to adjacent layers of fluid due to viscosity. Obviously the effect causes relative motion between solute and substrate, this may mean a resultant liquid flow (if the solid phase is immobile) or particle transport (if the liquid phase is immobile) or the motion of both phases. Figure 1 illustrates this mechanism.

A number of physical effects are closely related to EOF and are collectively known as ‘electro-kinetic effects’. The electro-kinetic phenomena can be divided into the following four categories (Probstein [8]):

(i) Electro-osmosis is the motion of ionized liquid relative to the stationary charged surface by an applied electric field,

(ii) Electrophoresis is the motion of the charged surfaces and macro-molecules relative to the stationary liquid by an applied electric field,

(iii) Streaming potential is the electric field created by the motion of ionized fluid along stationary charged surfaces (opposite of electro-osmosis) and

(iv) Sedimentation potential is the electric field created by the motion of charged particles relative to a stationary liquid (opposite of electrophoresis).

One of the earliest applications of EOF is in Civil Engineering as a method for drying soil. The application of a strong electric field to a porous media such as clay drives out water by electro-osmosis. The electrically driven flow of water can also be used to leach out contaminants in the soil in land reclamation projects (Probstein and Hicks [9]) or in the desalination of salt water (Probstein [10]). These early applications have now been completely eclipsed in due to the importance of modern applications in micro-fluidics.

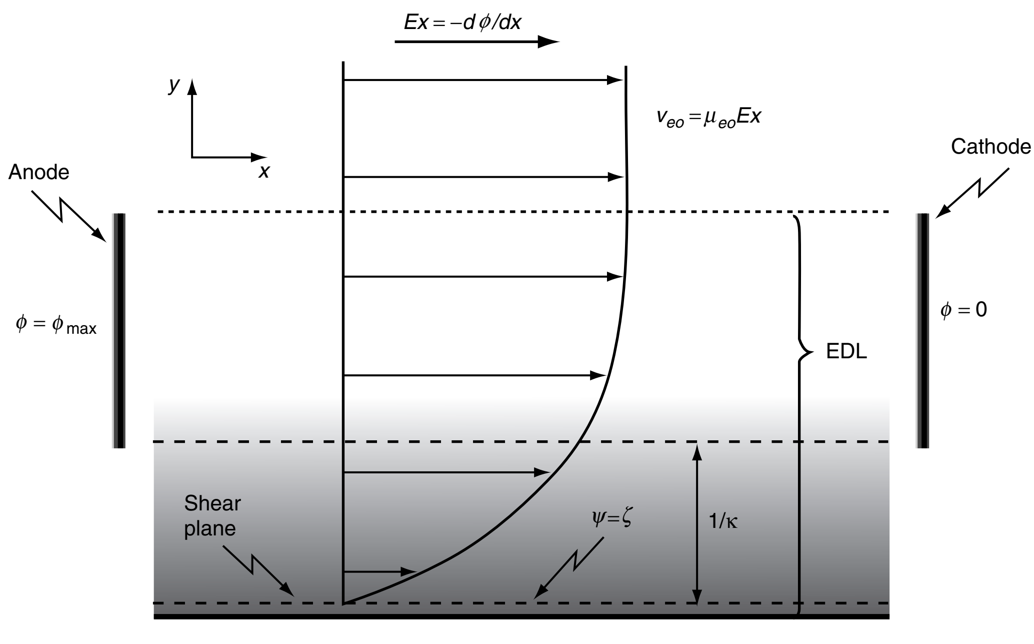

Figure 1. Electro-osmotic flow.

Electro-osmosis is defined as the process of inducing motion of ionized liquid relative to a stationary charged surface using an applied electric field. It describes the electrically-driven motion of fluid having net charge, which takes place in an electric boundary layer, called the Debye or electric double layer (hereinafter referred to as EDL), forming at the charged liquid/solid interface. It is the leading electro-kinetic phenomenon utilized in micro-fluidic systems. It enables fluid handling and flow control through selective applications of electric fields in micro-channel systems, eliminating moving mechanical components and significantly reducing mechanical failure modes due to fatigue and fabrication defects. Electro-osmotic pumping is commonly utilized in microchip-based sensors for detection of biological/chemical agents, and for various biomedical pumping and drug delivery applications.

Liquid flows in capillary porous systems under the influence of external electric fields have attracted the attention of many scientists, since the discovery of electro-kinetic transport by Reuss [7]. In 1870, Helmholtz developed the electric double layer theory, which relates the electrical and flow parameters for electro-kinetic transport. Electro-osmosis has also been used for chemistry applications since the late 1930's.

Theoretical developments include solution of mixed electro-osmotic/pressure driven flows in very thin two-dimensional slits (Burgreen and Nakache [11], Ohshima and Kondo [12], Dutta and Beskok [13]), as well as in thin cylindrical capillaries (Rice and Whitehead [14], Lo and Chan [15], Keh and Liu [16]. Overbeek [17] proposed irrotationality of internal electro-osmotic flows for arbitrarily shaped geometries. This is followed by the ideal electro-osmosis concept (i.e., electro-osmotic flow in the absence of externally imposed pressure forces) by Cummings *et al*. [18]. He has shown the similarity between the electric and velocity fields under specific outer field boundary conditions. More recently, Santiago [19] has shown that ideal electro-osmosis is observed for low Reynolds number, steady flows. However, unsteady or high Reynolds number flows violate this condition. Analytical solution of unsteady electro-osmotic flows obtained by Dutta and Beskok [20] confirms the predictions of Santiago [19].

The EOF velocity is given by the Helmholtz-Smoluchowski equation, $U = \dfrac{E\varepsilon\zeta}{\mu}$, where U represents

the velocity at the outer edge of EDL, ε is the permittivity of fluid, μ is the dynamic viscosity, E is the strength of the externally-applied electric field and ζ is the zeta potential defined as the induced electric potential at the Shear plane.

2. NUMERICAL METHODS

2.1. Governing equations

In this study the Gou-Chapman model is employed to describe the electro-osmosis. This section provides the governing equations that administer the momentum (flow process field), continuity and electricity (electric field) involved in the electro-osmotic flow. These equations form the basis of the theoretical modeling of pure electro-osmotic flow. They are

$$\frac{\partial u_i}{\partial t} + \frac{\partial u_i u_j}{\partial x_j} = -\frac{1}{\rho}\frac{\partial p}{\partial x_i} + \frac{\mu}{\rho}\frac{\partial^2 u_i}{\partial x_j \partial x_j} + \frac{\rho_e}{\rho}E_i + f_i \tag{1}$$

$$\frac{\partial u_i}{\partial x_i} - q = 0 \tag{2}$$

Where, $\dfrac{\rho_e}{\rho}E_i$ is are the electro-osmotic forcing component

This electric field, E is related to the externally applied electric potential by

$$E = -\nabla\phi \tag{3}$$

Here x_i's are the Cartesian coordinates, u_i's are the corresponding velocity components, f_i's are the momentum forcing components defined at the cell faces on the immersed boundary or inside the body,

μ is the fluid viscosity, ϕ is the external electric potential, ρ_e is the electric charge density and q is the mass source/sink defined at the cell center on the immersed boundary or inside the body. The governing equations for EOF are based on the following approximations:

(i) The fluid viscosity is independent of the shear rate assuming Newtonian fluid.
(ii) Ions are considered to be in equilibrium with the electric charge on the wall, thereby Poisson-Boltzmann equation is applicable for electro-kinetic potential distribution.
(iii) The solvent is continuous and its permittivity is not affected by the overall and local electric field strength.
(iv) The ions are point charges.
(v) Constant electric conductivity is assumed.

The EDL forms due to the interaction of an ionized solution with static charges on dielectric surfaces. The static charge on the surface influences distribution of ions in the buffer solution, which is determined by the Poisson-Boltzmann equation

$$\nabla^2\psi = -\frac{4\pi\rho_e}{D} \tag{4}$$

Where ψ is electro–osmotic potential , ρ_e is electric charge density and D is Dielectric constant.

In this equation $\rho_e = ze\ (C_p - C_m)$, where C_p is molar concentration of cation, C_m is molar concetration of anions, e is the electron charge and z is the valence.

Assuming boltzman distribution of the near charge surface

$$C_p = C_0 \exp\left[-\frac{ze\psi}{k_bT}\right] \tag{5}$$

$$C_m = C_0 \exp\left[\frac{ze\psi}{k_bT}\right] \tag{6}$$

$$\rho_e = -2zen_0 \sinh\left[\frac{ze\psi}{k_bT}\right] \tag{7}$$

Here n_0 is the bulk flow ion density, k_b is the boltzmann constant, T is the absolute temperature substituting various term on the right hand side of Eq. (4), it may be obtained as

$$\nabla^2\psi = \frac{8\pi zen_0}{D} \sinh\left[\frac{ze\psi}{k_bT}\right] \tag{8}$$

Conisdering a two-dimensionsal rectangular channel, it becomes

$$\frac{\partial^2\psi}{\partial x^2} + \frac{\partial^2\psi}{\partial y^2} = \frac{8\pi zen_0}{D} \sinh\left[\frac{ze\psi}{k_bT}\right] \tag{9}$$

To normalize the Eq. (9), following non-dimensional parameters are introduced:

$$x^* = \frac{x}{H}, y^* = \frac{y}{H}, \psi^* = \frac{\psi}{\zeta} \tag{10}$$

Where H is height of the microchannel (reference lenth) and ζ is the surface potential or wall potential. The nondimensional form of Eq. (9) is

$$\frac{\partial^2\psi^*}{\partial x^{*2}}+\frac{\partial^2\psi^*}{\partial y^{*2}}=\frac{H^2}{\zeta}\frac{8\pi zen_0}{D}\sinh\left[\frac{ze\zeta}{k_bT}\psi^*\right] \tag{11}$$

Difining the ionic energy parameter as

$$\alpha=\frac{ze\zeta}{k_bT} \tag{12}$$

and another non–dimensional parameter, β relating to α, ω and H can be obtained as

$$\beta=\frac{(\omega H)^2}{\alpha} \tag{13}$$

Here ω is the Debye Huckel parameter which is the reciprocal of EDL thickness λ

$$i.e.,\ \omega=\frac{1}{\lambda}=\sqrt{\frac{8\pi z^2e^2n_0}{Dk_bT}} \tag{14}$$

Eq. (11) may further written is non-dimensional form as follows

$$\frac{\partial^2\psi^*}{\partial x^{*2}}+\frac{\partial^2\psi^*}{\partial y^{*2}}=\beta\sinh\left[\alpha\psi^*\right] \tag{15}$$

2.1.1. Physical significance of α and β

At 20°C, ζ = 25.4 mV corresponds to α = 1. When the value of ζ is doubled, the value of α is equals 2 and so on.

If the channel height is 100 μm, the EDL thickness corresponding to different values of β is being depicted in Table 1. It is obvious that the thickness of EDL is increased as the value of β is increased.

Here ω is named as Debye–Huckel parameter, since $\frac{1}{\omega}$ gives characteristc thickness of EDL. The numerical solution of Eq. (15) is challenging due to the exponential non–linearity associated with hyperbolic sine function. Especially for large values of α, the non–linear forcing increasing for any

Table 1. Significance of β.

$\boldsymbol{\beta}$	**EDL thickness (μm)**	**EDL thickness as a fraction of channel height**
10000.0	1.0	1/100
1000.0	3.125	1/32
100.0	10.0	1/10
1.0	31.6	1/3.2

value of β, making the numerical solution challenging. For very large values of β when $\alpha = 1$, similar difficulties also exist. Accurate resolution of the problem requires high grid density within the EDL. Since $\lambda\left(=\frac{1}{\omega}\right)$ is proportional to $\frac{1}{\sqrt{\beta}}$, for constant value of α, lower value of β gives more EDL thickness. Higher value of β makes EDL thinner. Also $\lambda\left(=\frac{1}{\omega}\right)$ s proportional to $\frac{1}{\sqrt{\alpha}}$, for a constant value of β, lower value of α gives more EDL thickness. Higher value of α makes EDL thinner. Hyperbolic non–linearity can be tackled by Taylor series expansion (neglecting the higher order terms).

$$\sinh\left(\alpha\psi^*\right)^{n+1} = \sinh\left(\alpha\psi^*\right)^{n} + \left[\left(\alpha\psi^*\right)^{n+1} - \left(\alpha\psi^*\right)^{n}\right]\cosh\left(\alpha\psi^*\right)^{n} \tag{16}$$

Since mechanically driven parts are mostly bulky, many microfluidic related products which involve pressure driven forces have almost become obsolete in the last few years [21]. Hence, we only focus on microfluidic systems which use only electroosmotically driven forces in this article. Also the external electric field is applied at the inlet and outlet of the channel, the whole EOF may be assumed to be in stramwise direction and only the streamwise momentum equation is considered. That is, EOF is created by applying an external electric field. Here E is in the streamwise direction (i.e., $E = E_x$).

Substituting

$$\rho_e = -\frac{D}{4\pi}\left[\frac{\partial^2\psi}{\partial x^2} + \frac{\partial^2\psi}{\partial y^2}\right] \tag{17}$$

in Streamwise momentum equation, we have

$$\frac{\partial u}{\partial t} + \frac{\partial}{\partial x}\left(u^2\right) = \frac{\mu}{\rho}\left[\frac{\partial}{\partial x}\left(\frac{\partial u}{\partial x}\right) + \frac{\partial}{\partial y}\left(\frac{\partial u}{\partial y}\right)\right] - \frac{DE_x}{4\pi}\left[\frac{\partial^2\psi}{\partial x^2} + \frac{\partial^2\psi}{\partial y^2}\right] \tag{18}$$

Where permittivity $\varepsilon = \frac{D}{4\pi}$

To normalise the Eq. (18) the following non-dimensional parameter are introduced:

$$t^* = \frac{\mu t}{\rho H^2}, x^* = \frac{x}{H}, y^* = \frac{y}{H} \tag{19}$$

$$\psi^* = \frac{\psi}{\zeta}, u^* = \frac{u}{u_{ref}}, u_{ref} = -\frac{E_x\varepsilon\zeta}{\mu} \tag{20}$$

It is to be noted that the reference velocity is the Helmholtz-Smoluchowski electroosmotic velocity, $U = \frac{E\varepsilon\zeta}{\mu}$

$$\frac{\partial u^*}{\partial t^*} + \mathrm{Re}\left[\frac{\partial}{\partial x^*}\left(u^{*2}\right)\right] = \left[\frac{\partial^2 u^*}{\partial x^{*2}} + \frac{\partial^2 u^*}{\partial y^{*2}}\right] + \left[\frac{\partial^2\psi^*}{\partial x^{*2}} + \frac{\partial^2\psi^*}{\partial y^{*2}}\right] \tag{21}$$

Substituting Eq. (18) in Eq. (25),we have

$$\frac{\partial u^*}{\partial t^*} + \mathrm{Re}\left[\frac{\partial}{\partial x^*}\left(u^{*2}\right)\right] = \left[\frac{\partial^2 u^*}{\partial x^{*2}} + \frac{\partial^2 u^*}{\partial y^{*2}}\right] + \beta\sinh\left[\alpha\psi^*\right] \tag{22}$$

The Reynolds number range in electro-osmotic flow is between 0.0001 and 1.0. Hence the non-linear terms may be judiciously neglected. Equation (22) becomes

$$\frac{\partial u^*}{\partial t^*} = \left[\frac{\partial^2 u^*}{\partial x^{*2}} + \frac{\partial^2 u^*}{\partial y^{*2}}\right] + \beta \sinh\left[\alpha \psi^*\right] \tag{23}$$

2.2. Momentum forcing and interpolation for the velocity

The momentum forcing function is set into action (or introduced) whenever an immersed boundary is present and the same is applied only on the immersed boundary or inside the body. In the current study, a discrete-time momentum forcing function, f_i is introduced in to the Eq. (24) to mimic the no-slip condition. Thus the Eq. (23) becomes

$$\frac{\partial u^*}{\partial t^*} = \left[\frac{\partial^2 u^*}{\partial x^{*2}} + \frac{\partial^2 u^*}{\partial y^{*2}}\right] + \beta \sinh\left[\alpha \psi^*\right] + f_i \tag{24}$$

The forcing points are located at the grids where the streamwise component of the velocity is defined. To obtain u^*, from Eq. (25), the momentum forcing f_i must be determined in advance such that u^* satisfies the no-slip condition on the immersed boundary. When Eq. (25) is provisionally discretized explicitly in time to derive the momentum forcing value; by removing asterisks for the convenience, we have

$$\frac{\tilde{u}_{i,j}^{n} - u_{i,j}^{n-1}}{\Delta t} = \left[\frac{u_{i+1,j} - 2u_{i,j} - u_{i-1,j}}{\Delta x^2} + \frac{u_{i,j+1} - 2u_{i,j} - u_{i,j-1}}{\Delta y^2}\right] + \beta \sinh\left[\alpha \psi_{i,j}\right] + f_{i,j} \tag{25}$$

Rearranging Eq. (25) results in the following equation for $f_{i,j}$ at a forcing point,

$$f_{i,j} = \frac{U_{i,j}^{n} - u_{i,j}^{n-1}}{\Delta t} - \left[\frac{u_{i+1,j} - 2u_{i,j} - u_{i-1,j}}{\Delta x^2} + \frac{u_{i,j+1} - 2u_{i,j} - u_{i,j-1}}{\Delta y^2}\right] - \beta \sinh\left[\alpha \psi_{i,j}\right] \tag{26}$$

Here $U_{i,j}^n$ is the velocity to be obtained at a forcing point interms of $\tilde{u}_i^k$ through proper interpolation. $\tilde{u}_i^k$ indicates the velocity at a grid point nearby the forcing point updated from Eq. (25) with $f_{i,j} = 0$ to determine $U_{i,j}^n$ using linear interpolation.

In the case of no-slip wall, $U_{i,j}^n$ is zero as long as and when the forcing point coincides with the immersed boundary. However, in general the forcing point exists not on the immersed boundary but inside the body, and thus an interpolation procedure for the velocity $U_{i,j}^n$ is required. In the present study, second-order linear interpolations are used.

2.3. Mass source term

The procedure of obtaining the mass source q in Eq. (2) is generally explained in this section. Consider the two-dimensional cell shown in Fig. 2, where u_1 and v_1 are the velocity components inside the body and u_2 and v_2 are those outside the body. For the triangular cell containing only fluid ($\Delta P_B P_C P_D$), the continuity reads

$$u_2 \Delta y + v_2 \Delta x = 0 \tag{27}$$

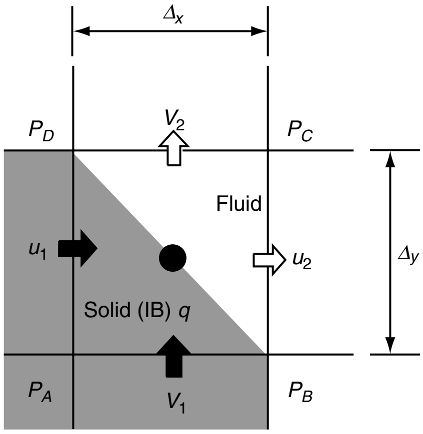

Figure 2. Mass conservation for a cell containing the immersed boundary.

Meanwhile, for the rectangular cell containing both the body and the fluid ($\Delta P_A P_B P_C P_D$) the continuity equation becomes

$$u_2 \Delta y + v_2 \Delta x = u_1 \Delta y + v_1 \Delta x + q \Delta x \Delta y \tag{28}$$

From Eq. (27) and Eq. (28), the mass source q is obtained as

$$q = -\frac{u_1}{\Delta x} - \frac{v_1}{\Delta y} \tag{29}$$

As we consider only the streamwise momentum equation, Eq. (29) will be modified as follows

$$q = -\frac{u_1}{\Delta x} \tag{30}$$

Near the immersed boundary, the velocities with and without q are fundamentally different from each other. Therefore the continuity equation along with mass source term in the vicinity of immersed boundary is

$$\frac{\partial u}{\partial x} + \frac{u}{\Delta x} = 0 \tag{31}$$

2.4. Geometry of the flow domain and boundary conditions

Figure 3 shows the two-dimensional channel with a patterned rectangular block having finite distance in between the channel, which is small compared to its length and width. Hence the flow through this channel is assumed to be two dimensional. The flow is assumed as unsteady and laminar. Also the

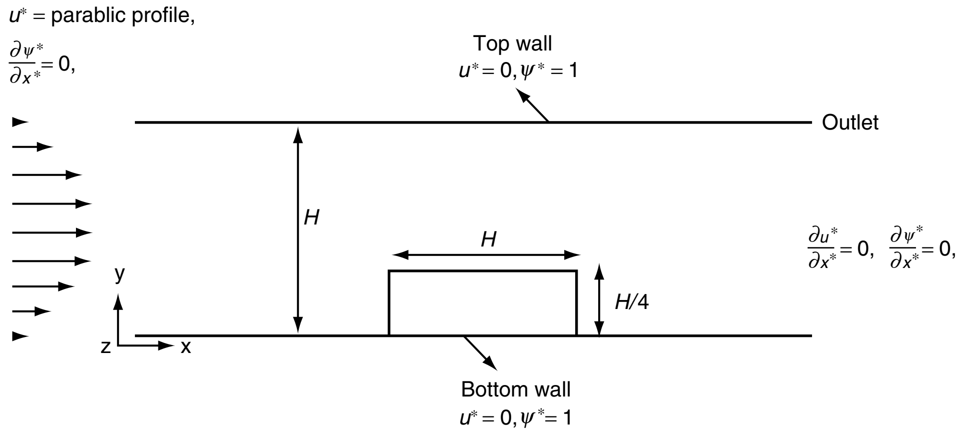

Figure 3. Schematic of the microchannel geometry for electroosmotic flow with a patterned rectangular block.

buoyant forces are negligible compared with viscous and pressure forces. The depicted boundary conditions in the respective figures are assumed for the computational simulation. Length to height ratio of the microchannel is arbitrarily assumed to be 5.

Inlet: In order to simulate a fully developed laminar micro-channel flow upstream of the block and to eliminate the corner effects, a standard parabolic velocity profile with a maximum velocity $u_{max} = (3/2)u_{ref}$ which is prescribed at the channel inlet for the present model.

Outlet: Fully developed velocity profile is assumed at the outlet and for non-dimensional electro-osmotic potential $\frac{\partial \psi^*}{\partial x^*} = 0$.

Walls: No slip condition for velocity. The non dimensional electro-osmotic potential is unity on all solid surfaces.

2.5. Solution procedure

For the spatial discretization of governing equations, a finite volume is employed. The Finite Volume Method (FVM) describes mass, momentum and energy conservation for solution of the set of differential equations considered for solving fluid flow problems. The FVM is considered to be more advantageous compared to other numerical methods, such as Finite Difference Method (FDM) and Finite Element Method (FEM). The FVM is characterized by the partition of the spatial domain in a finite number of elementary volumes for which are applied the balances of mass, momentum and energy. The approximated equations for the method can be obtained by two approaches. The first consists in applying balances for the elementary volumes (finite volumes), and the second consists in the integration of spatial-temporal of the conservation equations. In this work, the latter approach is followed.

Numerical solution of electroosmotic potential (Eq. (15)) with the help of Eq. (16) is fecilitated by point successive overrelaxation (PSOR) method. Solution of non-dimensional streamwise velocity component (Eq. (23)) is made possible by Alternating Direction Implicit (ADI) approximate factorization method clubbed with powerful and accurate Tri-Diagonal Matrix Algorithm (TDMA). Continuity is ensured by solving Eq. (31). The numerical code is developed using Digital Visual FORTRAN (DVF) and a detailed flow chart is shown in Fig. 4, based on which the computer code is developed.

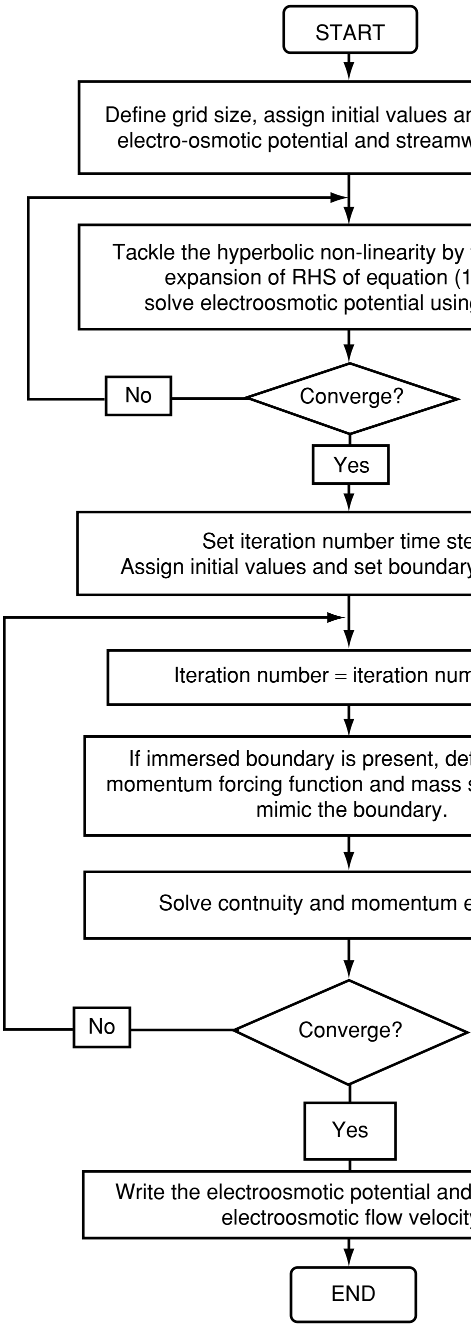

Figure 4. Flow chart to prepare the computer code.

3. RESULTS

Since the most significant area of micromixing studies is the flow analysis in various micro-channel configurations, the present results have major significance. An attempt is made here to simulate the electro-osmotic flow in a micro-channel with and without IB. It should be noted that the introduction of IB or obstacles in micro-channels definitely act as a flow control mechanism as well as a passive mixing enhancement technique. The results are generated with double precision. In order to ensure grid independency, extensive grid refinement studies were carried out for the computational geometry depicted in Fig. 3 (without rectangular block) for α = 1 and β = 10000. Considering the non-dimensional stream wise electroosmotic velocity at the centre of the channel outlet, it is seen that for the computational stencil of 251 × 101, percentage change of stream wise electroosmotic velocity with respect to previous stencil (201 × 81) is negligible.

This study commences by investigating the electroosmotic flow of a fluid in a microchannel shown in Fig. 3 without the rectangular block. It is noted that the height of the microchannel is given by H and that the length of the channel is denoted by L. The present simulation assumes the microchannel to be made of silica glass, to have a height of H = 100 μm and length of 500 μm and to possess a homogeneous zeta potential of ζ corresponding to the value of Ionic Energy Parameter, α. Furthermore, it is assumed that KCl electrolyte solution is used as the working fluid and that the physical properties of this solution are given by $\varepsilon = 80$, $\varepsilon_0 = 8.854 \times 10^{-3}$ $CV^{-1} \times m^{-1}$, $\mu = 0.90 \times 10^{-3}$ Nsm^{-2}. The results are generated first for the microchannel depicted in Fig. 2 without rectangular block for different values of α and β. There after a patterned rectangular block is immersed in the mingcrochannnel and is solved using IBM.

3.1. Verification of the code

To ensure the accuracy of the computed zeta potential distribution and the velocity profile, the numerical results are also compared along with the analytical results with respect to channel height presented in Patankar and Hu [21] and Yang *et al*. [22]. Here the analytical results are expressed interms of α and β in par with the present study. For the small zeta potential, Eq. 15 can be approximated by the first terms in a Taylor series. Thus, for the microchannel between two parallel flat plates, Eq. 15 can be reduced to

$$\frac{\partial^2 \psi^*}{\partial y^{*2}} = \alpha\beta\psi^* \tag{32}$$

The boundary conditions for the above equations are

$$\text{at } y^* = 0, \quad \psi^* = 1 \quad \text{and} \quad y^* = 1, \quad \psi^* = 1 \tag{33}$$

The solution is

$$\psi^* = \frac{\cosh\left[\sqrt{\alpha\beta}\left(y^* - 0.5\right)\right]}{\cosh\dfrac{\sqrt{\alpha\beta}}{2}} \tag{34}$$

In Fig. 5, numerical values of electroosmotic potential (wall potential) are plotted at the channel outlet and is compared with the analytical solution for β = 10000, β = 1000, β = 100, β = 10, β = 1 when α = 1. Clearly, the current solutions exacltly matches with the analytical solution. . For small values of β, the EDL is thick and it covers the entire channel. As the value of β is increased, the EDL is confined to the channel walls, resulting in sharp variations in the electric potential.

The nondimensional velocity distribution in the silicon microchannel can be computed by using Eq. (23). To ensure the numerical accuracy of solving the velocity field, we continue using the analytical results presented in Patankar and Hu [22] and Yang *et al*. [23]. The analytical solution for the velocity represents the steady-state solution in the fully developed region. The same is expressed in terms of α and β as follows

$$u^*\left(y^*\right) = 1 - \frac{\cosh\left[\sqrt{\alpha\beta}\left(y^* - 0.5\right)\right]}{\cosh\dfrac{\sqrt{\alpha\beta}}{2}} \tag{35}$$

Where y^* ranges from 0 to 1. Figure 6 plots the numerical values of electroosmotic velocity in the fully developed region compared with the analytical solution for β = 10000, β = 1000, β = 100, β = 10, β = 1 when α = 1. In this figure, it is clearly seen that the numerical results match very well with the analytical solution.

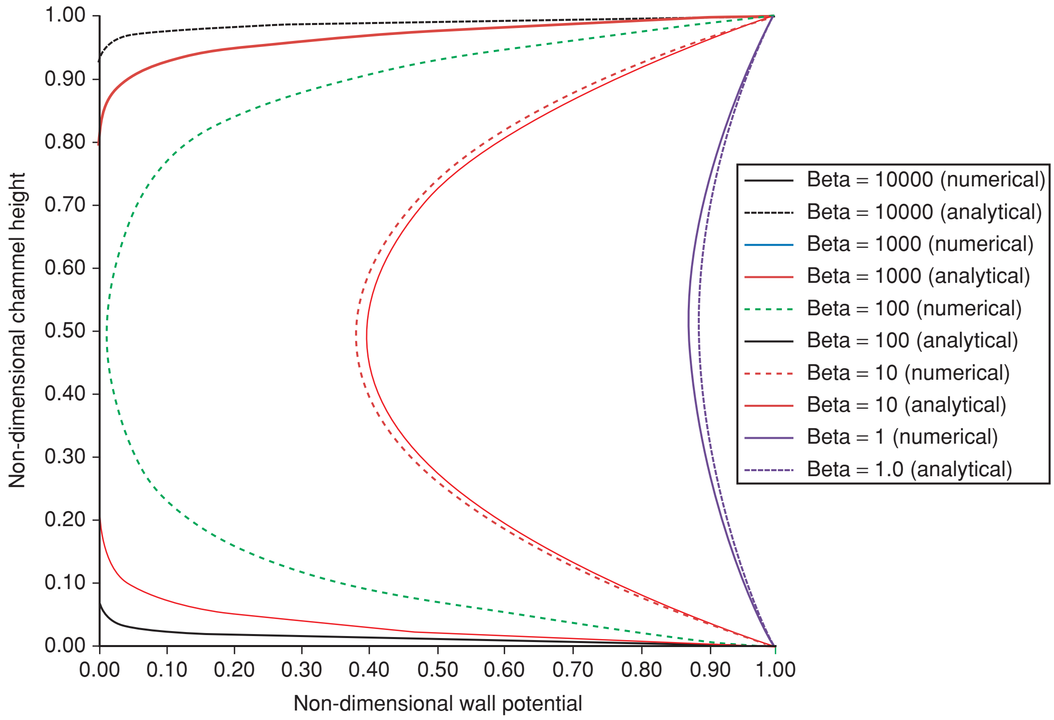

Figure 5. Variation of Electroosmotic Potential across the channel height.

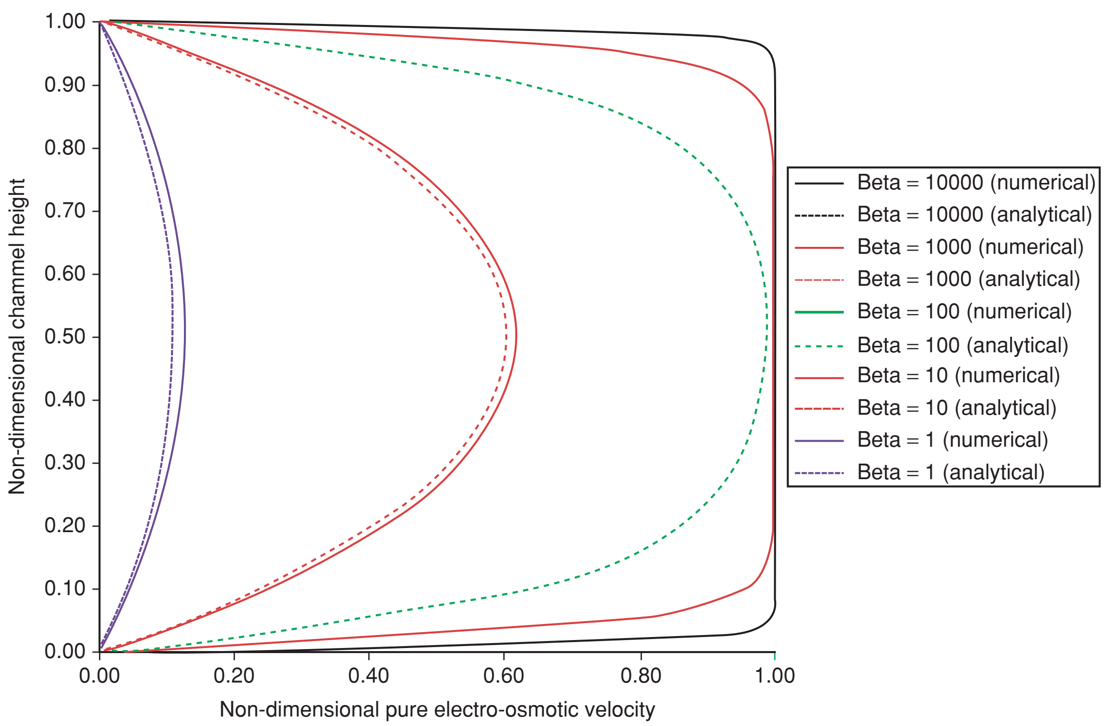

Figure 6. Variation of Electroosmotic Potential across the channel height for alpha = 1.

3.2. Electroosmotic flow

The electroosmotic flow is the fluid motion driven by an applied external electric field, which quite differs from the customary pressure-driven flow. The driving force is constant in the fully developed region for the pressure driven flow, when the velocity field is in a steady state. In classical fluid dynamics records many discussions in this regard can be found. In an electric-driven flow, an applied electric field acts on the net charge near the wall to produce a body force that drives fluid motion (This force is called the electroosmotic force). Figure 7 depicts the elecroosmotic potential contour in the microchannel for different values of β (10000, 1000,100,10 and 1) at $\alpha = 1$. In the electroosmotic

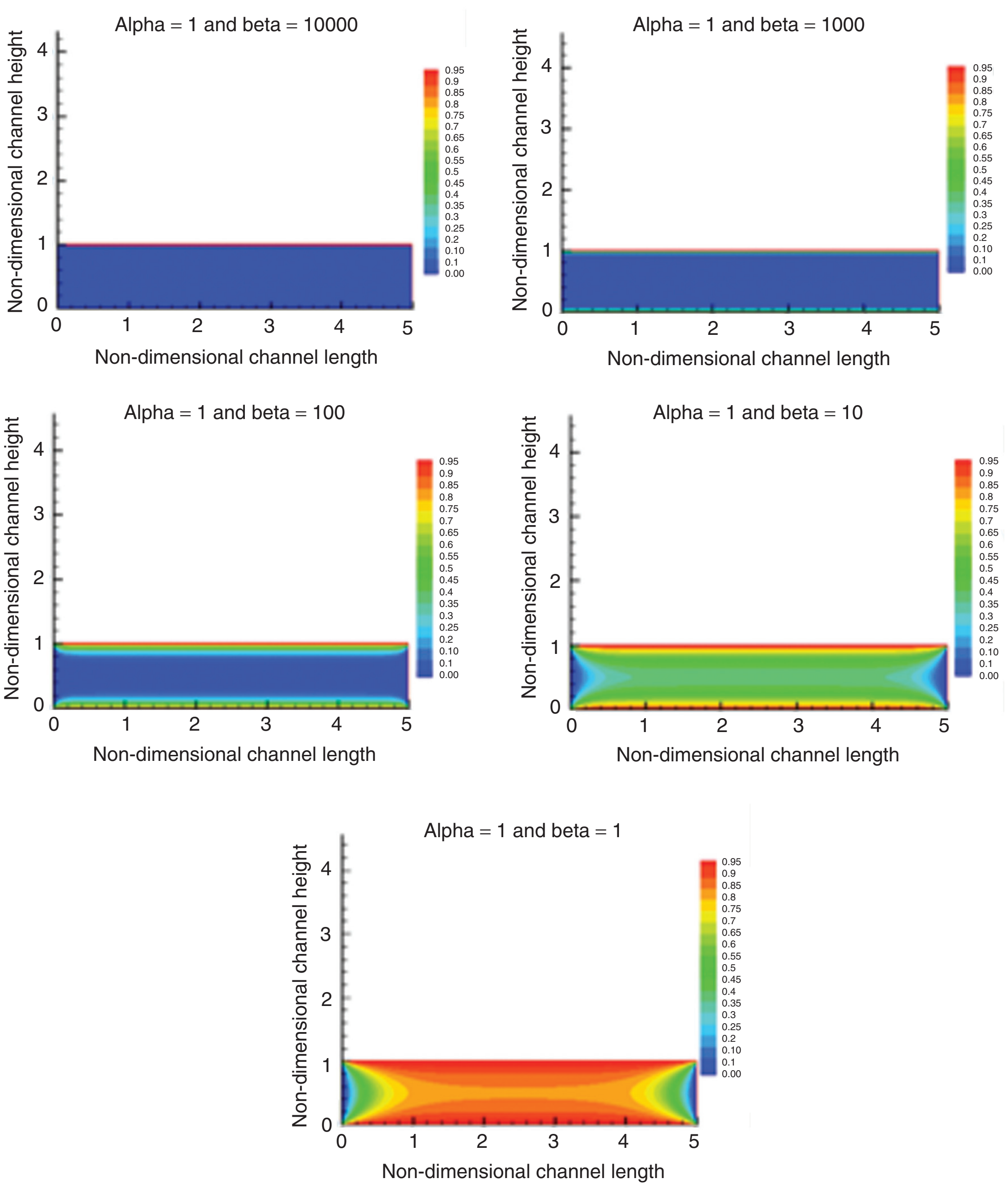

Figure 7. Electroosmotic Potential contour in the microchannel ($\alpha = 1$).

flow, the zeta potential of the channel wall influences the EDL distribution, and the potential is assumed to have a Gaussian distribution. In the Fig. 6, the reddish portion near the microchannel wall indicates the EDL. It is seen that the reddish colour gradually fills the channel as the value of the β decreases. Since the interaction between the fluid charge (ions) in the EDL near the wall and electric field is the important aspect driving the fluid motion, more fluid charge is ready to be attracted by external electric field when the thickness of EDL is increased. Thereby the deviation from plug shape to parabolic shape happens to the velocity contour as shown in Fig. 8. This figure furnishes the streamwise electroosmotic velocity contour in the microchannel for different values of β (10000, 1000,100,10 and 1) at $\alpha = 1$.

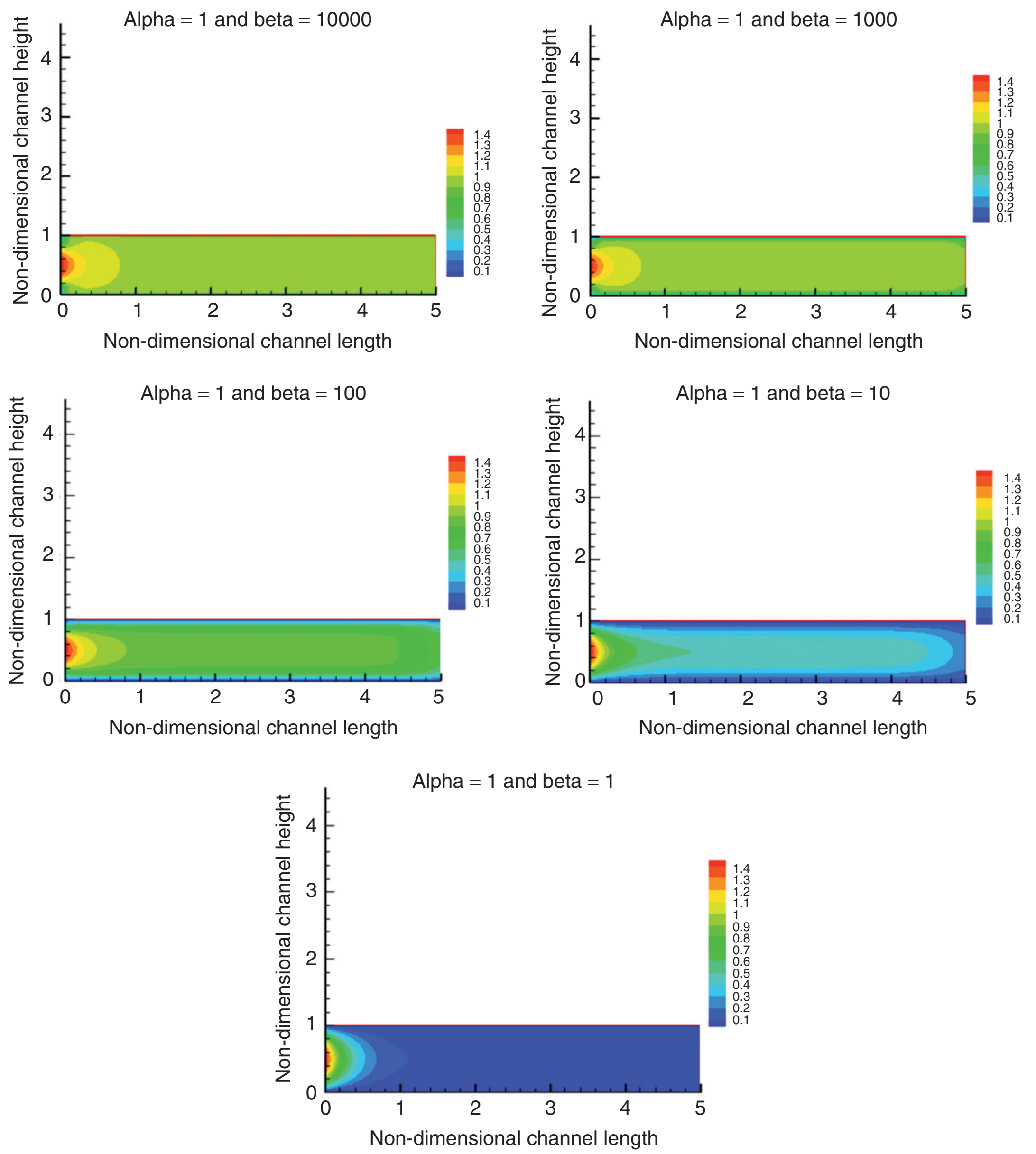

Figure 8. Streamwise component of electroosmotic flow velocity contours in the microchannel ($\alpha = 1$).

Further more as the thickness of the EDL increases corresponding to decreased value of β, the given external electric field which corresponds to a plug flow in a straight microchannel with identical length and electrochemical conditions is not sufficient to drag the fluid charge (ions) near the wall. Therefore, the magnitude of the electroosmotic velocity is deteriorating along the channel. Also the gradient of zeta potential is zero along the x direction, that is the direction along the microchannel wall as shown in Fig 7. The electroosmotic force is dominant in the vicinity of the wall region due to the contribution of β Sinh $(\alpha\psi^{*})$. This force is zero in the central region of the channel. The fluid motion in the central region is caused by viscous drag force.

Figure 9 shows the elecroosmotic potential contour in the microchannel for different values of β (β=10000, 10 and 1) at $\alpha = 10$. For a fixed value of β, comparisons of $\alpha = 1$ and $\alpha = 10$ curves show even faster decay of the electroosmotic potential for increased values of α. Figure 10 furnishes the streamwise electroosmotic velocity contour in the microchannel for different values of β (β =10000, 10 and 1) at $\alpha = 10$. The contour gradually deviates form a pure plug shape corresponding to $\beta = 10000$ to a deteriorated parabolic shape corresponding to $\beta = 1$. It can be understood from the velcoity contour that the flow is developed at a faster pace compared to velocity contour corresponding to $\alpha = 1$. This is because of the presence of more accumulation of fluid ions near the wall due to increase in thickness of EDL in par with $\alpha = 10$.

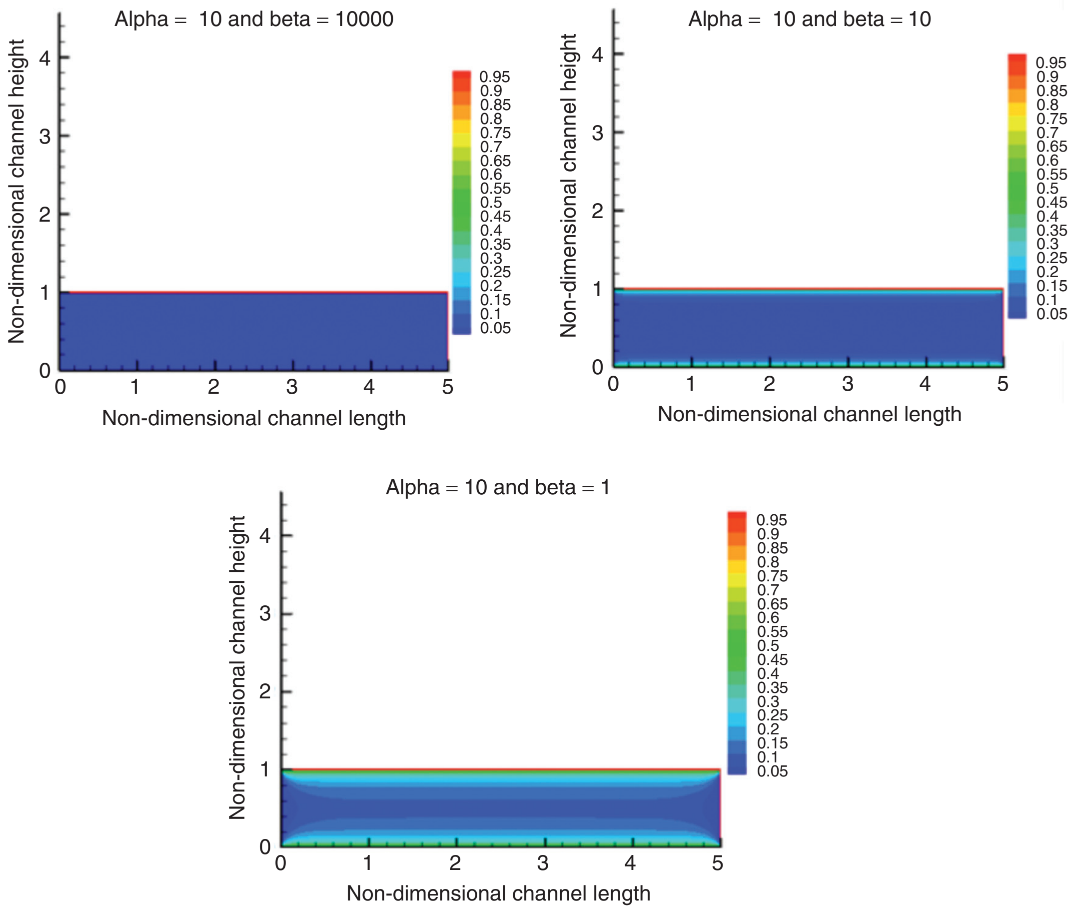

Figure 9. Electroosmotic potential contour in the microchannel ($\alpha = 10$).

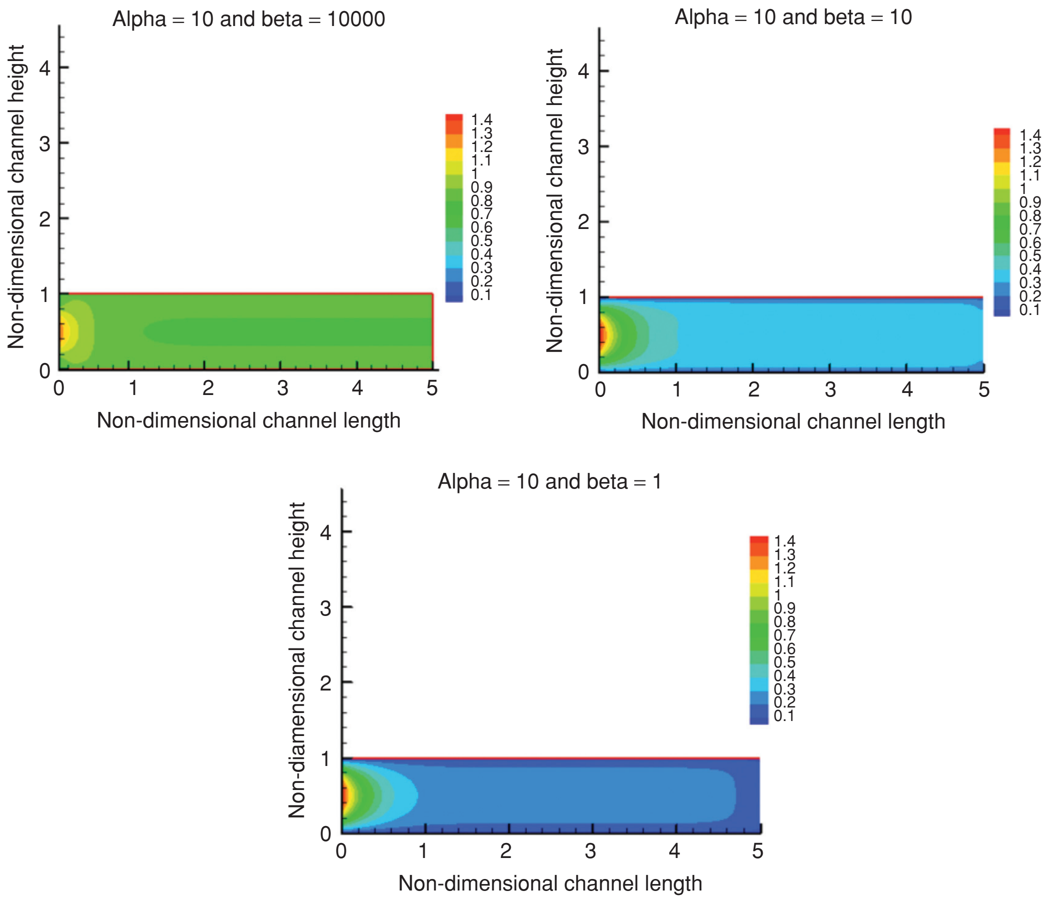

Figure 10. streamwise component of electroosmotic flow velocity contours in the microchannel ($\alpha = 10$).

3.3. Electroosmotic flow with immersed boundary

Electroosmotic flow in microchannels is usually restricted to low Reynolds number regimes characterized by extremely weak inertia forces and laminar flow. Subsequently, the mixing of dissimilar species occurs predominantly through diffusion, and hence cannot readily be accomplished within a short mixing channel. Here we presents a numerical exploration of electrokinetically driven flow in microchannels with a patterned rectangular blocks. The rectangular blocks are treated as immersed boundary and the solution is obtained by IBM. Here also the non-dimensional EDL and Navier-Stokes equations impregnated by momentum forcing functions were solved simultaneously to generate the electroosmotic potential and velocity contours. The simulation results confirm that the introduction of rectangular blocks within the microchannel. There is slight enhancement of species mixing. This is due to the constriction of bulk flow which is creating a stronger diffusion effect.

Figure 11 furnishes the electroosmotic potential contour in the microchannel with a rectangular block. As seen in this figure, the electric potential is maximum at the wall surface and drops off rapidly towards the channel centre. The pace of dropping off is decreased with decrease in value of β. At $\alpha = 1$ and $\beta = 10{,}000$, the electroosmotic potential drops to zero within the 1% of H. At $\alpha = 1$ and $\beta = 1000$, the electroosmotic potential drops to zero within the 3% of H. At $\alpha = 1$ and $\beta = 100$, the electroosmotic potential drops to zero within the 10% of H. At $\alpha = 1$ and $\beta = 1$, the electroosmotic potential drops to zero within the 31% of H. In all these cases, the contour lines are densely packed (red region in the plot) only next to the wall indicating a sharp decay in potential away from the walls. It is

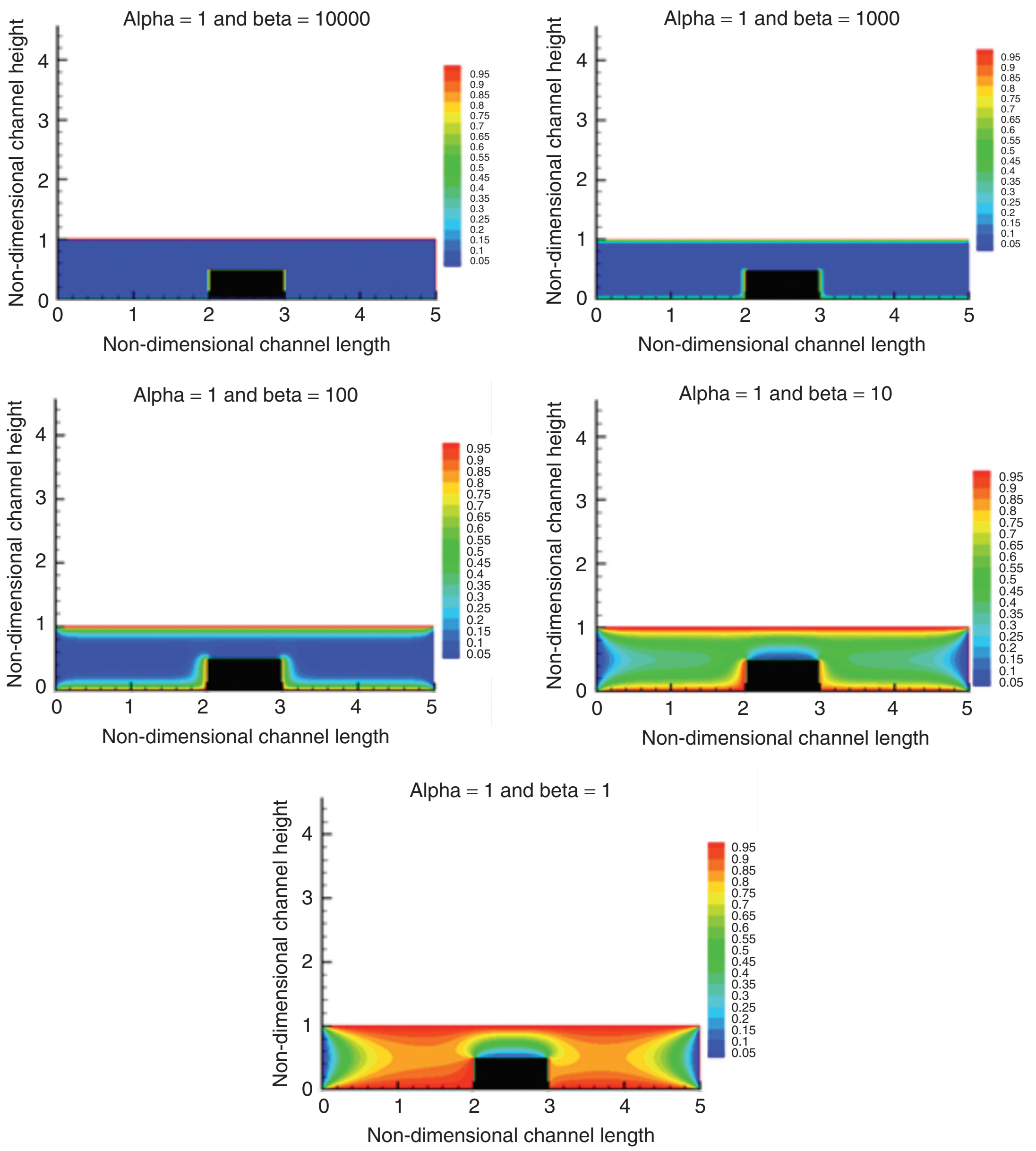

Figure 11. Electroosmotic potential contour in the microchannel with a rectangular block ($\alpha = 1$).

understood that the nature of the decay of electroosmotic potential is exponential and changes from a non-dimensional value of one at the walls to a value of zero away from the walls.

Figure 12 depicts the streamwise component of electroosmotic flow velocity contours in the microchannel with a rectangular block of length equals the height of the channel and height equals half of the channel height. Because of IBM, rectangular block in the flow field is considered a kind of momentum forcing in the Navier-Stokes equations rather than a treal body. Hence the rectangular block is easily handled without specifying the boundary conditions on the periphery of the block.

As expected, the presence of a large electroosmotic driving force near the channel wall causes the fluid particles to move initially in the EDL. The flow in this region which is tempted directly by the electric force can be observed as the active flow as indicated in the plots. Fluid velcoity increases

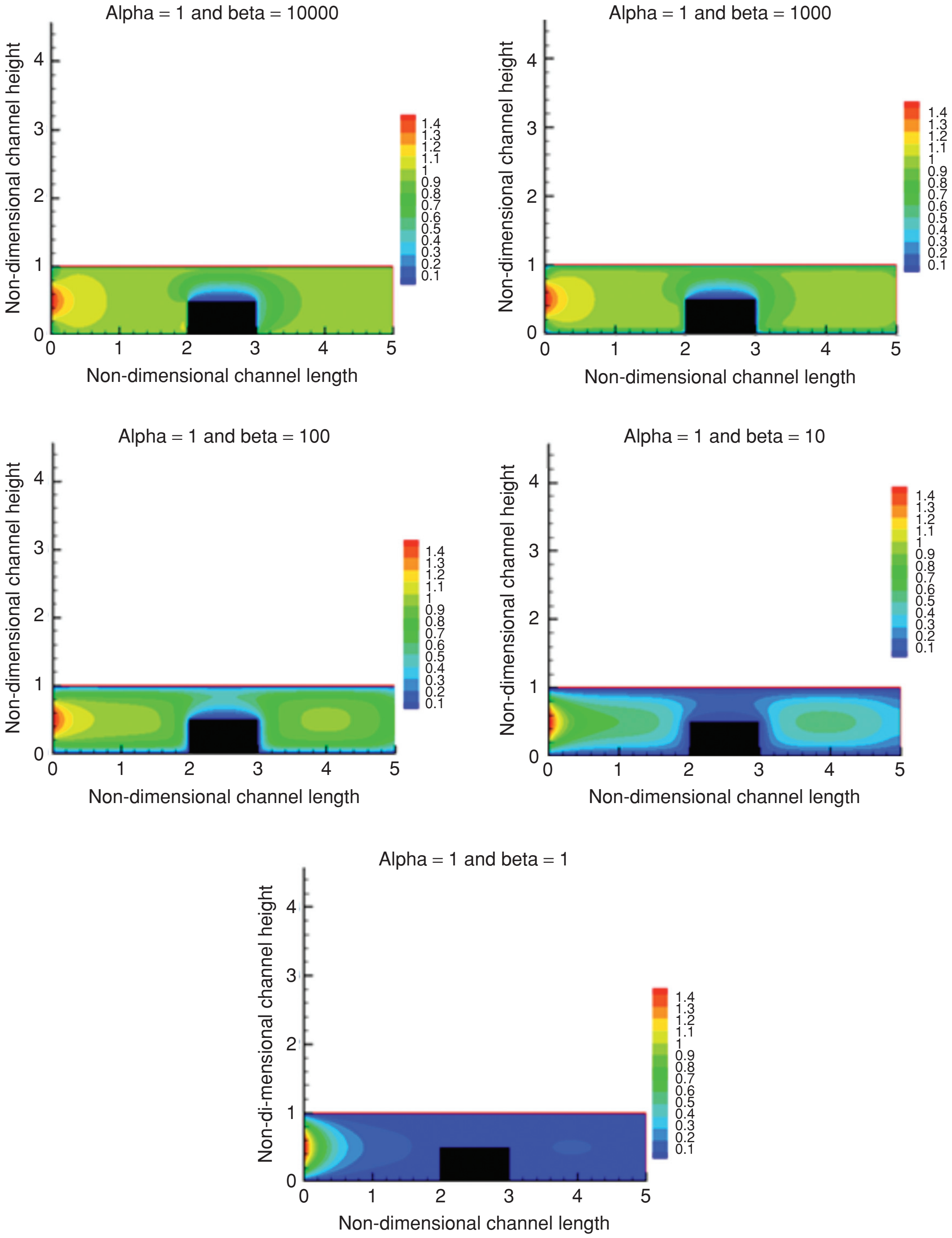

Figure 12. Streamwise electroosmotic flow velocity contours in the microchannel with an IB ($\alpha = 1$).

rapidly from zero at the wall (no slip condition) to a maximum near the wall, and as the time elapses, momenmtum is continuously transferred from the active layers to the central fluid until a steady state flow is attained maintaining the same value. The passive flow in the channel centre, which is caused by viscous drag forces, has a lower velocity compared with the active flow near the wall. Time taken to reach steady state is increasing with decrease of β values for a given α value. That is time to reach steady state at $\alpha = 1$ and $\beta = 10000$ is less compared to $\alpha = 1$ and $\beta = 1000$. Contours show that the non-dimensional level of the maximum velocity in the microchannel is of order one. The velcoity changes very abruptly adjacent the walls and stays persistent in the rest of the channel.

4. CONCLUSION

A numerical study of electroosmotic flow through a rectangular microchannels has been conducted in this study. A two-dimensional Poisson-Boltzmann equation which govern the electroosmotic potential (particularly EDL field) wholly in the rectangular microchannel is solved by the PSOR method. The hyperbolic non-linearity associated with this equation is suitably tackled by the Taylor series expansion (neglecting the higher order terms). Then two-dimensional Navier-Stokes equation in the rectangular microchannels are numerically solved by employing ADI approximate factorisation technique clubbed with powerful and accurate TDMA. Due to normalization of the above said governing equaions two parameters are defined (*viz*. α and β). Further, a patterned rectangular block is introduced to constrict the flow which eventually results in a short mixing channel. The introduced patterned rectangular block is treated by an IBM. The results are generated in terms of α and β.

REFERENCES

[1] F.H. Harlow, and J. E. Welch, Numerical calculation of time-dependent viscous of incompressible flow of fluid with free surface. Physics Fluids, 8, 2182–2189, 1965.

[2] C.S. Peskin, Flow patterns around heart valves: a numerical method, Journal of Computational Physics, 10, 252–271, 1972.

[3] R. Mittal, and G. Iaccarino, Immersed boundary methods, Annual Review of Fluid Mechanics, 37, 239–261, 2005.

[4] D. Goldstein, R. Handler, and L. Sirovich, Modeling a no-slip flow boundary with an external force field, J. Comp. Phys, 105, 354–366, 1993.

[5] M.J. Yusof, Combined Immersed-Boundary/B-Spline Methods for Simulations of Flow in Complex Geometries. Annual Research Briefs (Center for Turbulence Research, NASA Ames and Stanford University), 317–327, 1997.

[6] J. Kim, D. Kim, and H. Choi, An immersed-boundary finite-volume method for simulations of flow in complex geometries, Journal of Computational Physics, 171, 132–150, 2001.

[7] F.F. Reuss, Sur un nouvel effet de l'electricite galvanique, Memoires de la Societe Imperiale de Naturalistes de Moscou, 2, 327–337, 1809.

[8] R.F. Probstein, Physiochemical Hydrodynamics: An Introduction, New York: Wiley and Sons, 2nd edition, 1994.

[9] R.F. Probstein, and R.E. Hicks, Removal of contaminants from soils by electric fields, Science, 260, 498–503, 1993.

[10] R.F. Probstein, Desalination: Some fluid mechanical problems, Trans. ASME J. Basic Eng., 94, 286–313, 1972.

[11] D. Burgreen, and F.R. Nakache, Eletrokinetic flow in ultrafine capillary silts, J. Phys. Chem., 68(5), 1084–1091, 1964.

[12] H. Ohshima, and T. Kondo, Electrokinetic flow between two parallel plates with surface charge layers: Electroosmosis and streaming potential, J. Colloids and Interface Science, 135(2), 443–448, 1990.

[13] P. Dutta, and A. Beskok, Analytical solution of combined electroosmotic/ pressure driven flows in two-dimensional straight channels: Finite debye layer effects, Analytical Chemistry, 73, 1979–1986, 2001.

[14] C.L. Rice, and R. Whitehead, Electro kinetic flow in a narrow cylindrical capillary, J. Phys. Chem., 69 (11), 4017–4023, 1965.

[15] W.Y. Lo, and K. Chan, 1965, Poisson-Boltzmann calculations of ions in charged capillaris, J. of Chem. Phys.,. 69 (11), pp. 4017–4023, 1965.

[16] H.J. Keh, and Y.C. Liu, Electrokinetic flow in a circular capillary with a surface charge layer, J. Colloids and Interface Surfaces, 172, pp. 222–229, 1995.

[17] J.T.G. Overbeek, Colloid Science, Amsterdam: Elsevier Publishing Company, 1952.

[18] E.B. Cummings, S.K. Griffiths, R.H. Nilson, and P.H. Paul, Conditions for similitude between the fluid velocity and electric field in electroosmotic flow, Analytical Chemistry, 72(11), 2526–2532, 2000.

[19] J.G. Santiago, Electroosmotic flows in microchannels with finite inertial and pressure forces, Analytical Chemistry, 73(10), 2353–2365, 2001.

[20] P. Dutta, and A. Beskok, Analytical solution of time periodic electroosmotic flows: Analogies to Stokes' second problem, Analytical Chemistry, 73, 5097–5120, 2001.

[21] Chang C-C, Yang R-J (2006) A particle tracking method for analyzing chaotic electroosmotic flow mixing in 3-D microchannels with patterned charged surfaces. J Micromech Microeng 16: 1453–1462.

[22] N.A. Patankar, and H.H. Hu, Numerical simulation of Electro-osmotic flow, Analytical Chemistry, 70, 1870–1881, 1998.

[23] R.. J. Yang, L. M. Fu, and Y. C. Lin, Electroosmotic Flow in Microchannels, Journal of Colloid and Interface Science, 239, 98–105, 2001.